

## Role of Large Igneous Provinces in continental break-up varying from “Shirker” to “Producer”

Alexander Koptev <sup>1</sup>✉ & Sierd Cloetingh <sup>2</sup>

Traditionally, the emplacement of the Large Igneous Provinces (LIPs) is considered to have caused continental break-up. However, this does not always seem to be the case, as illustrated by, for example, the Siberian Traps, one of the most voluminous flood basalt events in Earth history, which was not followed by lithospheric rupture. Moreover, the classical model of purely active (plume-induced) rifting and continental break-up often fails to do justice to widely varying tectonic impacts of Phanerozoic LIPs. Here, we show that the role of the LIPs in rupture of the lithosphere ranges from initial dominance (e.g., Deccan LIP) to activation (e.g., Central Atlantic Magmatic Province, CAMP) or alignment (e.g., Afar LIP). A special case is the North Atlantic Igneous Province (NAIP), formed due to the “re-awakening” of the Iceland plume by the lateral propagation of the spreading ridge and the simultaneous approach of the plume conduit to adjacent segments of the thinner overlying lithosphere. The proposed new classification of LIPs may provide useful guidance for future research, particularly with respect to some inherent limitations of the common paradigm of purely passive continental break-up and the assumption of a direct link between internal mantle dynamics and the timing of near-surface magmatism.

**L**arge Igneous Provinces (LIPs) are defined as large volumes of predominantly mafic rocks characterized by a high rate of magma accumulation and unrelated to plate-tectonic processes, i.e., formed far away from plate boundaries within intraplate tectonic environments<sup>1–3</sup>. Within continents, such a sudden occurrence of continental flood volcanism is usually preceded by a rapid uplift of the surface topography of 0.5–2 km within a few Myr<sup>4,5</sup>. Most commonly, both the transient dome-shaped surface uplift<sup>6</sup> and the subsequent intraplate magmatic activity<sup>7</sup> are attributed to mantle plumes<sup>8</sup>, seismically detected thermal<sup>9,10</sup> or thermal–chemical<sup>11,12</sup> anomalies in the Earth’s mantle<sup>13,14</sup>. Importantly, these upwelling structures are not limited to the classic (“primary”) Morgan-type plumes<sup>15</sup> that rise from the mantle–core boundary (~2900 km) throughout the entire mantle but also include so-called “secondary” plumes<sup>16</sup> rooted in the upper-lower mantle transition zone (MTZ: ~410–660 km)<sup>17</sup>. Such small-scale anomalies in the upper mantle (also called “baby” plumes)<sup>18</sup> could originate from “primary” (super)plumes ponding at the 660 km phase change boundary<sup>19</sup> or be the result of deep dehydration of oceanic slabs stagnating in the lower part of the MTZ<sup>20–22</sup>.

Although the formation of LIPs is by definition not causally linked to plate-tectonic processes, Precambrian records in southern Africa show that LIPs may occur during supercontinental assembly<sup>23</sup> through thermal blanketing beneath the growing continent<sup>24</sup> and without support from mantle plumes<sup>25</sup>. In contrast, most Phanerozoic plume-related LIPs are known to be associated with the break-up of continents and the subsequent opening of large oceanic basins. This is evidenced by the spatial and temporal correlation between the major continental flood basalts formed in the last 300 Myr and the different phases of fragmentation of Pangea, the youngest supercontinent in Earth’s history<sup>26</sup> (see also Table 1). In addition, recent compilations

<sup>1</sup>GFZ German Research Centre for Geosciences, Potsdam, Germany. <sup>2</sup>Tectonics Research Group, Department of Earth Sciences, Utrecht University, Utrecht, Netherlands. ✉email: [alexander.koptev@gfz-potsdam.de](mailto:alexander.koptev@gfz-potsdam.de)

**Table 1 Break-up-based classification of Large Igneous Provinces (LIPs).**

LIP type	Examples		
	LIP and timing of emplacement	Separated continents and timing of break-up	Timing of pre-, syn-, and post-LIP continental rifting (or of attracted oceanic spreading)
<i>LIP-Shirker</i>	Siberian Traps [-250 Ma] <sup>40</sup>	-	West Siberian rift system <sup>a</sup> [-250–240 Ma] <sup>42</sup>
	Emeishan LIP [-260 Ma] <sup>47</sup>	-	Panxi rift <sup>a</sup> [-260–250 Ma] <sup>48</sup>
<i>LIP-Producer</i>	Madagascar LIP [-93–90 Ma] <sup>56</sup>	India–Madagascar [-84 Ma] <sup>66</sup>	Amirante pull-apart basin <sup>b</sup> [-95–85 Ma] <sup>74</sup>
	Deccan LIP [-66–64 Ma] <sup>57</sup>	India–Seychelles [-63 Ma] <sup>67</sup>	Cambay Basin, Kutch Basin, Narmada-Zone Rift <sup>b</sup> [-98.9–75 Ma] <sup>75–77</sup>
<i>LIP-Trigger</i>	Central Atlantic Magmatic Province (CAMP) [-201 Ma] <sup>98</sup>	Africa–North America [-190 Ma] <sup>107</sup>	Central Atlantic rift system <sup>c</sup> [since -225 Ma] <sup>104</sup>
	Karoo LIP [-184–182 Ma] <sup>99</sup>	Africa–Antarctica/Madagascar [-168–164 Ma] <sup>108</sup>	Karoo rift system <sup>c</sup> [since -190 Ma] <sup>106</sup>
<i>LIP-Attractor</i>	Afar LIP [-30 Ma] <sup>121</sup>	Africa–Arabia [-19–17 Ma] <sup>119</sup>	Carlsberg Ridge <sup>d</sup> [since -63 Ma] <sup>67</sup>
	Paraná–Etendeka LIP [-134–132 Ma] <sup>126</sup>	Africa–South America [-133–125 Ma] <sup>125</sup>	South Atlantic Ridge <sup>d</sup> [since -133 Ma] <sup>125</sup>
<i>LIP-Dornröschen</i>	North-Atlantic Igneous Province (NAIP) <sup>e</sup> [-62–58 Ma] <sup>142</sup>	North America–Greenland [-64–56 Ma] <sup>143,144</sup>	Labrador Sea Ridge <sup>d</sup> [since -64 Ma] <sup>143</sup>
		Greenland–Europe [-54–53 Ma] <sup>145</sup>	Norwegian–Greenland Sea rift <sup>c</sup> [since >300 Ma] <sup>166</sup>
<i>LIP-Sleeper</i>	Manus Basin (Western Pacific) <sup>172</sup>	-	-

<sup>a</sup>LIP-induced aborted rift(s).

<sup>b</sup>Pre-LIP extensional basin/rift oblique to future syn-LIP magmatic break-up trend.

<sup>c</sup>Pre-LIP rift system evolving into break-up after LIP emplacement.

<sup>d</sup>Remote center of oceanic spreading propagating toward LIP-induced lithospheric soft point.

<sup>e</sup>LIP emplacement delayed by several tens Myr in relation to plume arrival time.

of continental and oceanic LIPs (including those found not only on the present-day seafloor but also in ophiolites) have shown a statistical correlation between the number of mantle plume events and supercontinental cycles since >1000 Myr<sup>27</sup>.

However, the concept of plume-induced continental rupture can be challenged by the following observations: (1) long-lasting (up to ~200 Myr) phases of near-amagmatic rifting preceding emplacement of LIPs<sup>28</sup> and (2) the coincidence of the location and orientation of break-up axes with pre-existing suture zones<sup>29</sup>. In conjunction with arguments in favor of low (50–100 K) potential temperature anomalies beneath commonly accepted mantle plumes, such as the Iceland plume<sup>30</sup>, not only has the active role of LIPs in Pangea break-up<sup>31</sup> been questioned, but even the existence of mantle plumes themselves<sup>32,33</sup>. It should be noted that all of these “anti-plume” views are generally at odds with deep mantle geochemical signatures of the LIPs<sup>34</sup> and other volcanic hotspot lavas<sup>35</sup>.

To reconcile these apparent contradictions between active (driven by mantle plumes) and passive (driven by far-field tectonic forces) mechanisms of continental rifting and subsequent break-up, attempts have been made to develop transitional<sup>36</sup> or combined<sup>37–39</sup> passive-active scenarios. More recently, intermediate types of rifting-to-break-up systems (such as the so-called “semi-active” and “semi-passive”) have also been identified<sup>18</sup>. With this in mind, we examine major continental LIPs emplaced since the Late Paleozoic and propose a new classification consistent with their relationship to the disintegration of Pangea.

**LIPs without break-up (*LIP-Shirker*).** We begin our overview of Phanerozoic LIPs with two examples that, contrary to common expectations, are completely ineffective in terms of continental

break-up and subsequent onset of oceanic spreading. Therefore, we refer to this type of LIP as *LIP-Shirker*.

The Permo-Triassic Siberian Traps (~250 Ma<sup>40</sup>) is an archetypal example of a continental LIP (Fig. 1a), best known for its proven impact on the largest known mass extinction event<sup>11,41</sup>. Despite the concurrent development of a rift system beneath the West Siberian Basin<sup>42,43</sup>, one of the largest hydrocarbon provinces in the world<sup>44,45</sup>, the Siberian Traps did not result in plate rupture and subsequent formation of an ocean basin.

Coincidence or not, another *LIP-Shirker* developed around the same time: the Late Permian (~260 Ma) Emeishan LIP was emplaced on the western margin of the Yangtze Cratonic block of South-West China<sup>46,47</sup>. Similar to the Siberian Traps, the Emeishan LIP was accompanied by plume-induced continental rifting<sup>6,48</sup>, which took place in the Panxi region above the plume head<sup>49</sup>, possibly also in the presence of far- and near-field tectonic stresses<sup>50</sup>.

These two examples document that without appropriate geodynamic conditions (e.g., the presence of a pre-existing weak zone at the site of LIP emplacement and/or high-level and long-lasting far-field extensional stresses), even the most voluminous extrusions of flood basalts are insufficient to cause continental break-up with their impact limited to aborted rift systems.

Although the criteria for defining LIPs are not quite met, the Tertiary volcanic provinces of western and central Europe are probably another example of a “*Shirker*”. In this case, the European Cenozoic Rift System (ECRIS) was likely activated during the Paleogene<sup>51</sup> by a mantle plume or a system of small (“secondary”) plumes that have been magmatically active since the Paleocene<sup>52</sup> and can still be detected through seismic tomography<sup>53,54</sup>. The change in geodynamic regime at ~35 Ma

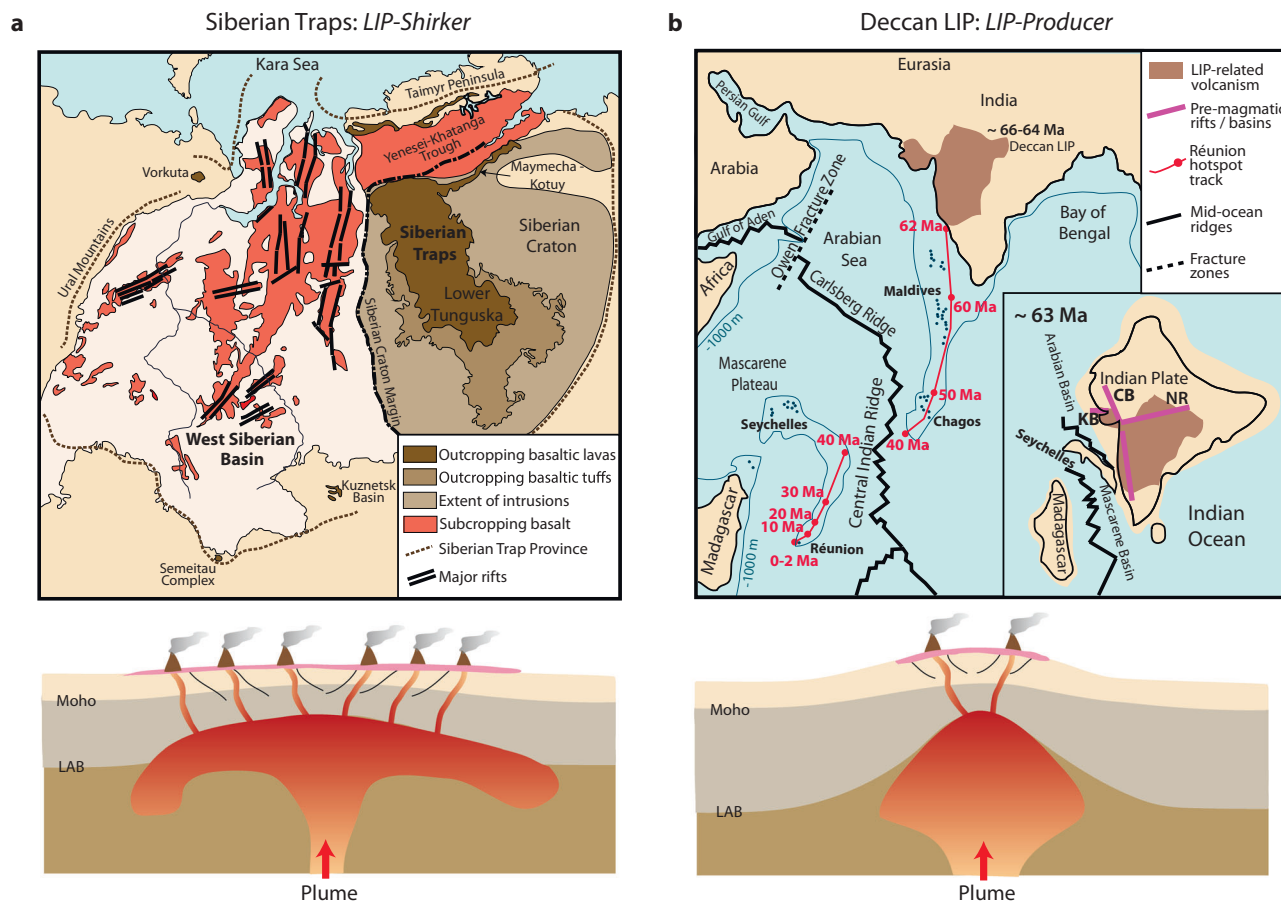


**Fig. 1 End-member LIP types.** **a** Siberian Traps as an example of *LIP-Shirker*. Hot upwelling material spreads laterally below the lithosphere-asthenosphere boundary (LAB) to form a mushroom-shaped plume head feeding widespread magmatic activity over an area of up to  $\sim 5.0 \times 10^6$  km<sup>2</sup>. Plume-induced continental rifting (the West Siberian rift system) terminated in  $\sim 10$  Myr during the Middle Triassic<sup>42</sup> without rupturing the lithosphere. Geological map is modified from ref. <sup>40</sup>. **b** Deccan LIP as an example of *LIP-Producer*. Rapid penetration of the mantle plume through the lithospheric mantle, which is progressively thinned in the active-passive mode<sup>37,79</sup>, leads to continental break-up shortly after (in a few Myr) emplacement of LIP-related volcanism, which in this case is much more spatially restricted, covering an area of  $\sim 1.5 \times 10^6$  km<sup>2</sup>. Réunion hotspot track is after refs. <sup>70,71</sup>. Paleo-position of the Seychelles microcontinent at  $\sim 63$  Ma is after ref. <sup>67</sup>. Note the oblique orientation of the pre-magmatic rifts/basins (CB—Cambay Basin; KB—Kutch Basin; NR—Narmada-Zone Rift)<sup>75–77</sup> with respect to the break-up axis (future Carlsberg Ridge) between the Indian Plate and the Seychelles<sup>78</sup>.

(transition from progressive closure of the Neo-Tethys Ocean to development of back-arc basins over retreating slabs)<sup>55</sup> has aborted the ECRIS and made the European volcanic province an equivalent counterpart to the more voluminous *LIP-Shirkers* discussed above.

**LIPs with break-up.** In contrast to the *LIP-Shirker* end-member, most cases of LIP emplacement result not only in rifting but also in rupture of the continental lithosphere<sup>26</sup>. Considering the relative role of mantle plumes associated with LIPs in the break-up process, we introduce the following types: *LIP-Producer*, *LIP-Trigger*, and *LIP-Attractor*. Their characteristic features are described below along with the natural examples and the criteria for distinguishing them.

**LIP-Producer.** The *LIP-Producer* corresponds to a scenario in which plume emplacement determines the location and timing of continental rupture. Prominent examples are the Madagascar and Deccan LIPs (Fig. 1b), where the rapid eruption of intraplate flood basalts occurred at  $\sim 93$ – $90$  Ma<sup>56</sup> and  $\sim 66$ – $64$  Ma<sup>57</sup>, respectively. The continental lithosphere overlying the corresponding mantle plumes was therefore effectively weakened by basal thermo-mechanical erosion<sup>58–60</sup> and the reduction in the long-

term brittle strength of rocks exposed to melt percolation<sup>61–63</sup>. In addition, this weakened lithosphere was subjected to slab pull forces by the continuous subduction of the Neo-Tethys Ocean floor<sup>64</sup>, sometimes enhanced by a double subduction with two nearly parallel, north-dipping subduction zones between the Indian and Eurasian plates<sup>65</sup>. Under such favorable conditions, corresponding to the active-passive scenario when the mantle plume is combined with far-field tectonic extension<sup>37–39</sup>, the continents were broken-up in only a few Myr after the formation of the Madagascar and Deccan LIPs, resulting in the successful separation of Madagascar and India at  $\sim 84$  Ma<sup>66</sup> and India and the Seychelles at  $\sim 63$  Ma<sup>67</sup>. Consistent with the classic concept that flood basalts represent the “head” of the plume and that continued magmatism along hotspot tracks is associated with the remaining plume “tail”<sup>68</sup>, the Madagascar and Deccan LIPs mark the spatial and temporal beginning of well-known oceanic hotspot tracks that terminate at the current position of the Marion<sup>69</sup> and Réunion<sup>70–72</sup> plumes, respectively. It is also important that the Mesozoic extensional basins that preceded the emplacement of both the Madagascar<sup>73,74</sup> and Deccan LIP<sup>75–77</sup> are characterized by a strong obliquity with respect to the future break-up axis<sup>78</sup>.

As evident from these examples, on the one hand, the role of the *LIP-Producer* is dominant because plate-tectonic forces alone

(e.g., slab pull by long-lived subduction since the Paleozoic)<sup>64</sup> were not sufficient to localize rifting at the site and with the same orientation as the axis of eventual break-up. On the other hand, as shown by contrary *LIP-Shirker* end-member cases (Siberian Traps and Emeishan LIP), complete rupture of the lithosphere would not be possible without appropriate (extensional) far-field stresses determining the orientation of the break-up axis<sup>79,80</sup>. Paradoxically, the East African Rift System (EARS) could be an example of both end-members. The ongoing purely active rifting in its Eastern Branch, established in the Miocene<sup>81</sup> after the emplacement of the Kenya plume<sup>82–85</sup> at ~40–45 Ma<sup>86</sup>, did not yet evolve into the rupture of the African Plate. Obviously, this is due to an unfavorable tectonic setting with regional far-field compression by mid-ocean ridges surrounding the African continent<sup>87–89</sup>. In the absence of a plate-tectonic reorganization, the EARS will be aborted, similar to the fate of the ECRIS and other rift systems associated with *LIP-Shirkers*. In an opposite scenario where a switch in the tectonic regime can make break-up possible, the East African volcanic province will be an equivalent of *LIP-Producer*.

Importantly, mantle plume impingement can produce not only (super)continent rupture, but also the separation of relatively small continental ribbons or microcontinents<sup>90,91</sup>. In particular, several continental fragments are known to have drifted away from northern Gondwana during the Paleozoic (the Avalonia terranes and the Cimmerian blocks)<sup>92</sup> and Mesozoic (the Apulian microcontinent)<sup>93</sup>, possibly due to the combined effect of slab pull by continuous subduction of paleo-oceans (from Proto-Tethys to Neo-Tethys)<sup>94</sup> beneath the active margin of opposing continents (from Laurentia to Laurasia)<sup>95</sup> and mantle plumes periodically arriving at the base of the African lithosphere<sup>96</sup>.

*LIP-Trigger*. In contrast to the *LIP-Producer* scenario, where thermal and magmatic weakening caused by a mantle plume leads to initial localization of pre-break-up deformation in the lithosphere, the magmatic activity associated with an *LIP-Trigger* is preceded by continental rifting, situated in the area of future lithospheric rupture and, crucially, of the same orientation as the final break-up axis<sup>78</sup>. Prominent examples are the Central Atlantic Magmatic Province (CAMP) and the Karoo LIP, emplaced at ~201<sup>97,98</sup> and ~184–182 Ma<sup>99–102</sup>, respectively. In these cases, the role of the corresponding plumes was limited, only enhancing the ongoing localized extension related to pre-magmatic rifting which in both regions was already operating for several tens<sup>103,104</sup> to several<sup>105,106</sup> Myr. Therefore, the CAMP and the Karoo LIP activated (but did not cause!) lithospheric rupture that occurred relatively soon (~10–15 Myr) after their emplacement, opening the Central Atlantic at ~190 Ma<sup>107</sup> and separating South Africa from Antarctica and Madagascar at ~168–164 Ma<sup>108</sup>.

We dub this type of LIP as *LIP-Trigger* because in this case pre-LIP localized deformation (rifting) could ultimately be terminated by a break-up of the continent, even without the involvement of a plume that merely accelerates (or triggers) this process without playing a dominant role. Coincidence or not, both *LIP-Triggers* (the CAMP and the Karoo LIP) lack hotspot tracks, unlike the *LIP-Producers* (the Deccan and Madagascar LIPs), which, as described above, have a clear expression in the form of tracks imprinted by deep-seated Réunion and Morion plumes. Therefore, *LIP-Triggers* seem to be preferably associated with bundles of “secondary” plumes rather than with individual “primary” plumes (Fig. 2a). This assumption is indirectly supported by (1) the presence of numerous small plumes in the central Atlantic Ocean (Azores, Canary, and Cape Verde)<sup>109</sup>, which are obviously much younger (Cenozoic) in age<sup>110,111</sup>, but could indicate a “secondary” plume fabric, that established in the region during the Late Triassic–Early Jurassic and is still in operation; (2) a larger area of scattered magmatism associated with *LIP-Triggers*

(e.g., ~3 × 10<sup>6</sup> km<sup>2</sup> for the Karoo LIP) than in the case of a spatially more concentrated magmatic area typical of *LIP-Producers* (e.g., ~1.5 × 10<sup>6</sup> km<sup>2</sup> for the Deccan LIP); and (3) strong multivariance in proposed positions for the center of the Karoo plume<sup>112</sup>. We should note, however, that despite our hypothesis of numerous “secondary” plumes below the CAMP and the Karoo LIP this is not a general requirement for the *LIP-Trigger*, which in principle can also develop with a single “primary” plume, as exemplified by the Kerguelen oceanic plateau formed in the Early Cretaceous as a LIP over the Kerguelen hotspot<sup>113</sup>. The first magmatism associated with the Kerguelen plume has been dated to ~130 Ma in southwestern Australia<sup>114</sup> and ~132 Ma in southeastern Tibet<sup>115</sup>, roughly contemporaneous with the initial break-up of India–Antarctica<sup>116</sup> and India–Australia<sup>117</sup>, which in turn was preceded in both cases by continental rifting since ~160 Ma<sup>118</sup>, consistent with the *LIP-Trigger* scenario.

*LIP-Attractor*. For both *LIP-Producer* and *LIP-Trigger*, continental break-up always occurs first above the plume emplacement area, forming volcanic passive margins (VPMs), and then propagates laterally, developing non-volcanic passive margins (NVPMs), which are usually abruptly separated from volcanic counterparts by transform faults<sup>78</sup>. On the contrary, in the case of the Afar LIP (Fig. 2b), the NVPMs at the eastern tip of the Gulf of Aden began to develop much earlier (~19–17 Ma<sup>119</sup>) than the VPM formation within the Afar triple junction (~1 Ma<sup>120</sup>). This spatial and temporal evolution of the break-up of the Gulf of Aden could be explained as follows: a domain of the continental lithosphere, that was rheologically weakened by the massive melting event of the Afar plume at ~30 Ma<sup>121,122</sup>, directed the westward lateral propagation of seafloor spreading from the mid-oceanic Carlsberg Ridge, which had already been active since ~63 Ma<sup>67</sup> and then approached this thermal sublithospheric anomaly acting as a soft point<sup>123</sup>. We, therefore, dub this type of LIP as *LIP-Attractor*.

In the South Atlantic<sup>124</sup>, break-up at 133–125 Ma<sup>125</sup> also propagated (in this case from south to north) toward the Paraná-Etchedeka LIP, which erupted almost simultaneously at ~134–132 Ma<sup>126</sup>. This sequence has been hypothesized as evidence for a non-plume mechanism of South Atlantic opening<sup>127</sup> and Pangea fragmentation in general<sup>31</sup>. However, it is more likely that we are dealing here with another *LIP-Attractor*, where the influence of the plume is restricted to directing the propagation of oceanic spreading that is already operating.

It should be mentioned that from the perspective of the opening of the Red Sea, the Afar LIP can also be considered as *LIP-Producer*. In this case, initial continental rifting occurred almost simultaneously with plume emplacement<sup>119</sup>, while the break-up was considerably delayed until ~4 Ma at the southern tip, without yet reaching the northern segments of the Red Sea<sup>128</sup>. This delay between the LIP formation and the resulting plate rupture (not typical of the classic *LIP-Producers*, where break-up usually develops much more rapidly) may be due to a much reduced Neo-Tethys slab pull since the onset of the progressive collision between the Arabian and Eurasian Plates in the Bitlis suture zone at ~40–30 Ma<sup>129</sup>. Consequently, it appears that in the classic active–passive scenarios corresponding to the *LIP-Producers*, the time interval between LIP emplacement and final break-up is controlled primarily by a combination of the efficiency of lithosphere weakening by magmatism (volume, temperature, and water content of plume material) and the level of external extensional forces.

**“Re-awakened” and “dormant” LIPs (*LIP-Dornröschen* and *LIP-Sleeper*).** Despite decades of extensive study and the

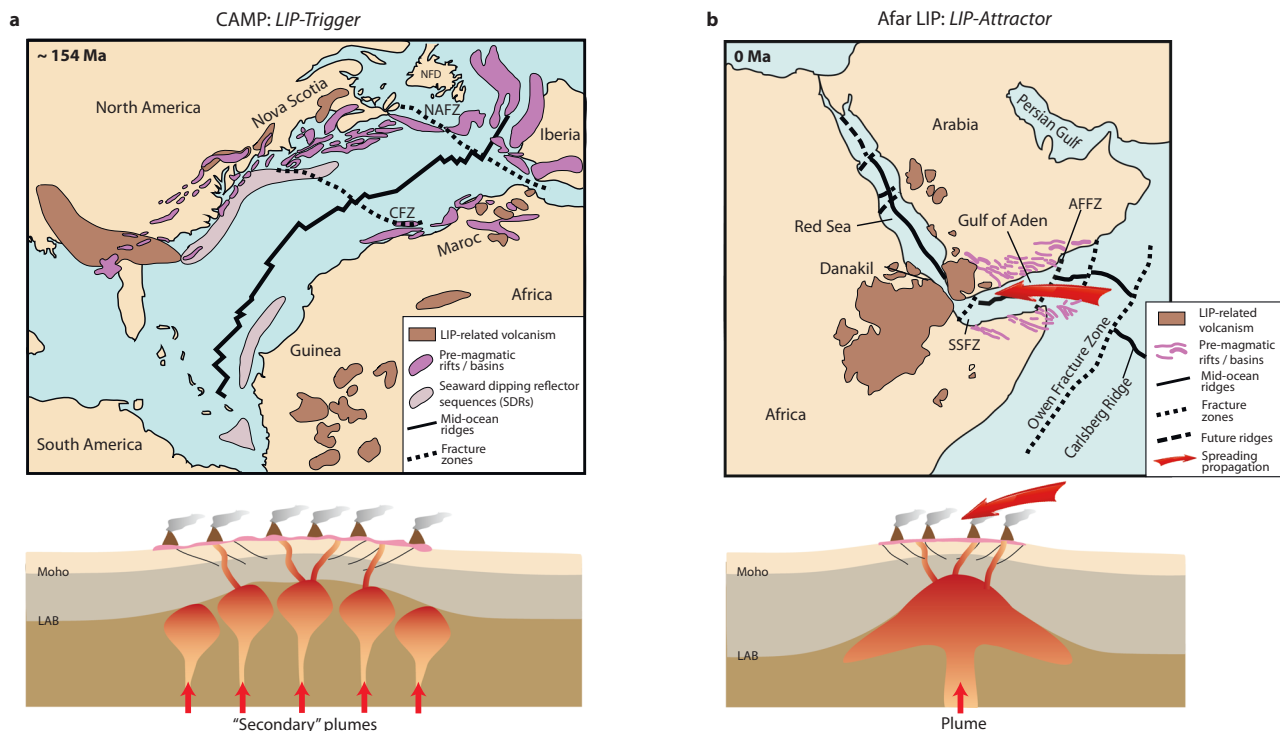


**Fig. 2 Other types of LIPs associated with break-up.** **a** Central Atlantic Magmatic Province (CAMP) as an example of *LIP-Trigger*. Simultaneous emplacement of numerous “secondary” plumes<sup>16</sup> at the base of the pre-thinned lithosphere results in scattered magmatism that is relatively quickly followed (in  $\sim 10$  Myr) by plate rupture. Concentrated volcanism coincident with plume-related lithospheric break-up forms large and thick wedges of so-called seaward dipping reflector sequences (SDRs) that mark volcanic passive margins (VPMs), in contrast to adjacent non-volcanic passive margins (NVPMs) without SDRs that presumably develop as part of a purely passive rifting-to-break-up system. Note that the VPMs of the Central Atlantic are separated from the NVPMs between Newfoundland and Iberia by a series of major transform faults. CFZ Canary Fracture Zone, NAFZ Newfoundland-Azores Fracture Zone, NFD Newfoundland. **b** Afar LIP as an example of *LIP-Attractor*. Soft point in the lithosphere created by plume-induced thermal anomaly at  $\sim 30$  Ma<sup>121,122</sup> controls the direction of horizontal propagation from the Carlsberg Ridge, which causes progressive break-up in the Gulf of Aden from the east ( $\sim 19$ – $17$  Ma)<sup>119</sup> to the west ( $\sim 1$  Ma)<sup>120</sup>. AFFZ Alula-Fartak Fracture Zone, SSFZ Shukra El Sheik Fracture Zone. Two maps in **a** and **b** are modified from ref. 78.

accumulation of a vast amount of geologic and geophysical data<sup>130</sup>, the North Atlantic Igneous Province (NAIP) and the associated evolution of lithospheric rupture and oceanic spreading are still the subject of vigorous debate about the mechanisms that favor either plume-induced<sup>131,132</sup> or purely passive rifting and break-up<sup>133</sup>.

To reconcile ongoing controversies about the actual causes of the emplacement of voluminous magmatism in the NAIP, the following key elements of the evolution and structure of the North Atlantic realm should be taken into account as constraints: (1) the spatial variation in the thickness of the continental lithosphere<sup>134–136</sup>; (2) the relative motion trajectory of the Iceland plume since the Cretaceous<sup>137–139</sup>; (3) the timing and spatial distribution of the magmatism related to the NAIP<sup>140–142</sup>; and (4) the timing of the opening of the Labrador Sea/Baffin Bay<sup>143,144</sup> and the North Atlantic<sup>145,146</sup>. According to these data, the lithosphere is thinned beneath the central part of Greenland, as evidenced by low seismic velocities in the mantle<sup>134–136</sup>. This seismically detected zone of relatively thin lithosphere crossing Greenland from west to east is also reflected in high measured<sup>147</sup> and predicted<sup>148</sup> heat flow, intense basal ice melt<sup>149</sup>, and increased crustal thickness due to magmatic underplating<sup>150</sup> and intrusions in the middle and lower crust<sup>151</sup>. Given the spatial correspondence with the reconstructed paths of the Iceland hotspot<sup>137–139</sup>, most recent studies interpret these features as relict signatures of the passage of the Iceland plume beneath Greenland from at least 90 to  $\sim 60$  Ma<sup>148–151</sup>. In contrast, according to more traditional views, the Iceland plume

was emplaced on the eastern edge of Greenland, as supported by observations of radiating and circumferential dyke swarms<sup>152</sup>, whereas part of its large, flattened head rapidly extended into western Greenland<sup>153</sup>, causing the quasi-simultaneous magmatic activity (the NAIP) on both sides of Greenland around 60 Ma<sup>140–142</sup>. However, the relatively close location of the reconstructed position ( $\sim 130$ – $120$  Ma) of the so-called High Arctic Large Igneous Province, which includes the exposed components on Ellesmere Island, Spitsbergen, and perhaps northern Greenland<sup>154</sup>, and the corresponding segment of the hotspot track<sup>132</sup> is indicative of the Iceland plume, which is more than twice as old as the NAIP<sup>137</sup>. Furthermore, the Iceland hotspot can even be traced back to West Siberia in the Late Permian–Early Triassic<sup>155</sup>, so that the Siberian Traps ( $\sim 250$  Ma<sup>40</sup>) could hypothetically be the very first magmatic manifestation of the Iceland plume.

In view of the above, magmatic activity in Baffin Island and Western Greenland during the Paleocene was probably triggered by spreading axis propagation from the Labrador Sea toward the Baffin Bay, where continental break-up was progressively initiated from  $\sim 64$  Ma<sup>143</sup> to  $\sim 56$  Ma<sup>144</sup>, respectively. The overlap of the propagating spreading ridge with the  $\sim 100$ – $80$  Ma-dated segment of the Iceland hotspot track near the West Greenland passive margin<sup>139</sup> (Fig. 3a) enlivened the hot material that had resided there already for  $\sim 20$ – $40$  Myr without signs of excessive volcanism. The simultaneous approach of the actual “tail” of the Iceland plume to the eastern edge of thick Greenland lithosphere<sup>139</sup> allowed horizontal flow of the plume material

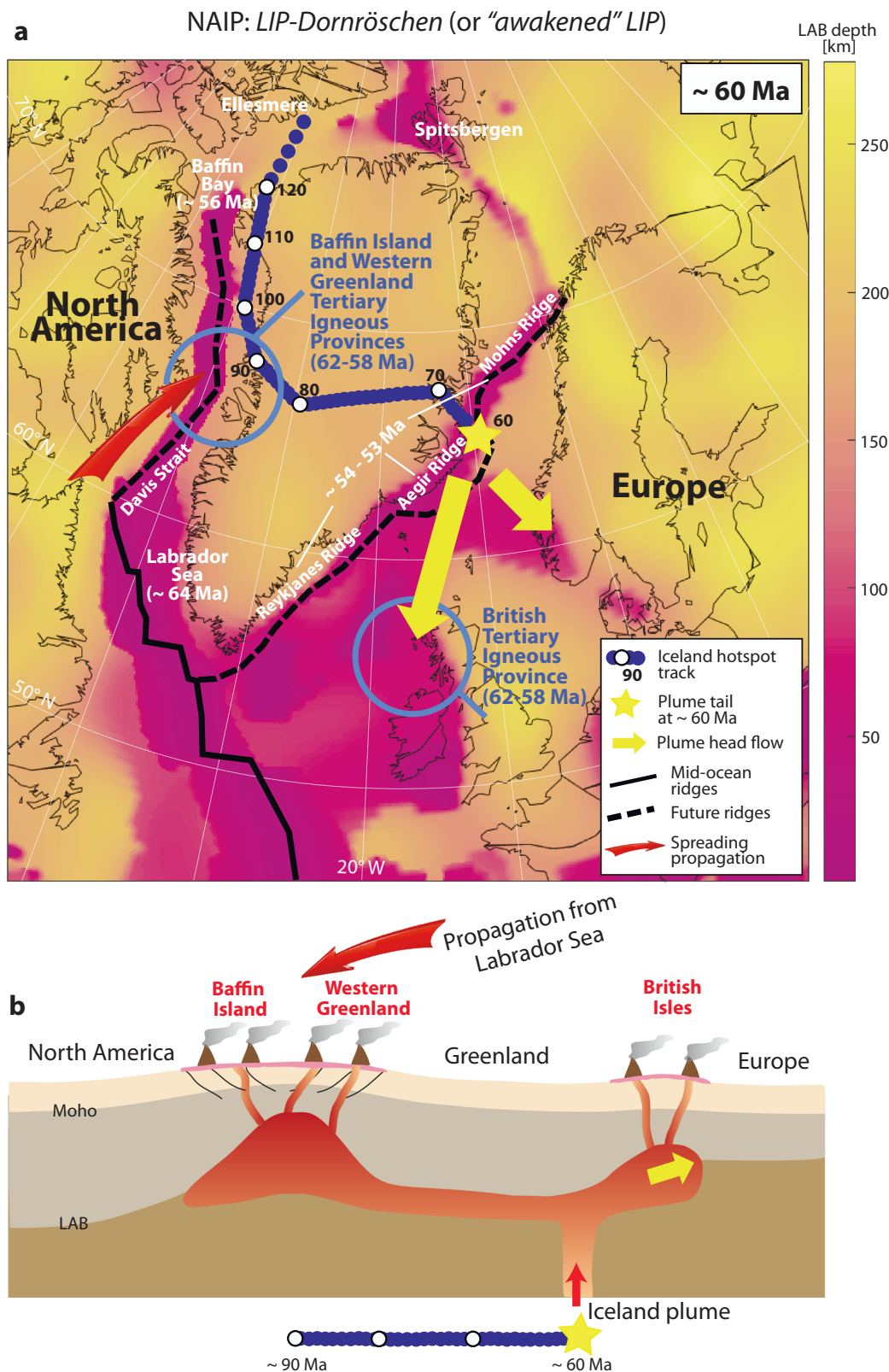


**Fig. 3 North Atlantic Igneous Province (NAIP) as an example of LIP-Dornröschen (or “re-awakened” LIP).** **a** Thickness of continental lithosphere (LAB depth), based on seismic tomography model by ref. <sup>135</sup>. A ~60 Ma plate reconstruction and the Iceland plume trajectory are based on the global moving hotspot reference frame of ref. <sup>139</sup>. Blue circles indicate the approximate location of two NAIP regions. **b** Schematic profile showing: (1) “re-awakening” of plume material seeded since ~90 Ma on the western edge of Greenland by propagation of the spreading axis from the Labrador Sea, and (2) flow of hot material delivered from the plume source on the eastern edge of Greenland toward the thinner lithosphere of Europe. These independent but coincident events led to the simultaneous (at ~62–58 Ma)<sup>142</sup> emplacement of the Baffin Island/West Greenland and British Tertiary Igneous Provinces, which together form the NAIP. Note that the vertical scale is exaggerated on this and other (Figs. 1 and 2) schematic profiles. Map in **a** is modified from ref. <sup>132</sup>.

along the adjacent thin-lithosphere corridors<sup>135</sup> connecting the eastern edge of Greenland with the Southern Scandinavia and Scotland/Ireland<sup>156,157</sup>. A similar mechanism of propagation of hot plume material toward areas distant from its original emplacement along the elevated lithosphere–asthenosphere boundary<sup>158–160</sup> has been proposed for Late Mesoproterozoic mafic magmatism in the southwestern USA (the Keweenaw LIP and the Southwest Laurentia LIP)<sup>161</sup> and Cenozoic alkaline volcanism in Africa<sup>162</sup> and Arabia<sup>163,164</sup>. The arrival of Iceland plume hot material beneath thin European lithospheric segments has led to intense plume-related magmatism in the British Isles area<sup>165</sup>, quickly followed by the break-up in the North Atlantic *sensu stricto* (i.e., between Greenland and Europe) along the Reykjanes–Aegir–Mohns Ridge at ~54–53 Ma<sup>145</sup>, preceded by the most long-lasting rifting since the Late Paleozoic<sup>166,167</sup>. The contemporaneous (~62–58 Ma) magmatism over a vast area from Baffin Island to the British Isles<sup>142</sup> is thus driven by these two independent processes—spreading axis propagation and plume conduit motion—which happen to coincide in time (Fig. 3b).

The evolution of the North Atlantic region shows that a thermal anomaly hidden for a while beneath thick lithosphere can be “re-awakened” (or “re-initialized”) by the lateral propagation of spreading ridges or by tapping its source under thinner segments of overlying lithosphere due to horizontal plate movements. We dub this type of LIPs as *LIP-Dornröschen* (“re-awakened” LIP). We expect that the term *LIP-Dornröschen* (*LIP-Sleeping Beauty*) may be applicable to a broad family of LIPs, including those from the Precambrian. For example, several LIP pulses in the period 1800–1600 Ma, which formed on the supercontinent Columbia during ancient plate motion over a single stationary Xiong’er plume in the North China Craton<sup>168</sup>, can be regarded as the earliest known manifestation of a *LIP-Dornröschen*-like scenario in Earth history. On the contrary, the youngest case of delayed LIP outpouring might be the Columbia River Basalt LIP (~17–16 Ma<sup>169</sup>) associated with the Yellowstone mantle plume<sup>170</sup>, with a history appearing to extend to at least ~56 Ma, as indicated by offshore volcanism on the Siletzia oceanic plateau<sup>171</sup>.

Interestingly, the western (Baffin Island and Western Greenland) and eastern (British Isles) components of the North Atlantic “Sleeping Beauty” show some similarities to the *LIP-Attractor* and the *LIP-Trigger*, respectively (see Fig. 3 and Table 1), so a multilevel classification for these and/or other LIPs (and/or LIPs components) could probably be developed in the future.

The mantle plume underlying the Manus back-arc basin (Western Pacific Ocean), which was discovered by seismic tomography without showing up as an evident hotspot<sup>172</sup>, is likely a good example of a possible future *LIP-Dornröschen* that is currently still “dormant” (*LIP-Sleeper*). Future high-resolution seismic tomographic studies in continental and oceanic lithospheric environments will be of particular importance in discovering new “dormant” plumes or hidden hotspots<sup>173</sup>, which may provide additional constraints on plate motion history<sup>174</sup> and will likely help uncover new aspects in the geodynamics of mantle-lithosphere interactions.

**Conclusions and future outlooks.** For more than 25 years, the prevailing view of the scientific community on the causal links between mantle plumes and the break-up of (super)continents has changed considerably. Traditionally, it was postulated that the emplacement of LIPs played a key role in Pangea fragmentation<sup>26</sup>. However, recognition of certain limitations of this concept<sup>28,29</sup> has gradually led to a fundamental reassessment of the causes of continental break-up<sup>31</sup>, which ultimately rules out the necessity<sup>175</sup> and even the existence of a mantle plume component<sup>32,33</sup>. As a

consequence, purely passive continental rifting models are now even being applied to regions such as East Africa<sup>176–179</sup>, where both geophysical<sup>83,85</sup> and geochemical<sup>82,84</sup> observations unequivocally indicate the presence of mantle plumes, rooted in a common large-scale source corresponding to a first-order mantle structure such as the African superplume<sup>180,181</sup>.

To prevent further counterproductive discussions advocating end-member views of classic “passive versus active” rifting debate<sup>182</sup>, a parallel of the more general “plates versus plumes” controversy<sup>32,33</sup>, we propose here a new classification of LIPs that illustrates the variability in the possible role of mantle plumes in the process of continental break-up (in addition to the well-known diversity in geochemically based classifications)<sup>23,183</sup>. In particular, we demonstrate that, on the one hand, LIPs indeed cannot always be causally linked to lithospheric rupture. As the geologic records of the Siberian Traps and the Emeishan LIP (*LIP-Shirkers*) show, even very voluminous magmatism associated with active rifting does not always by itself lead to continental break-up in the absence of favorable tectonic conditions. On the other hand, regional far-field extension alone also does not act as an efficient break-up mechanism, as most non-volcanic passive margins (e.g., Newfoundland–Iberia, Equatorial Atlantic) are the result of horizontal propagation from adjacent areas of plume-activated spreading<sup>78</sup>. This highlights the key role of combined active–passive mechanisms<sup>38,184</sup>, where the site of localized deformation is determined by the plume, while the orientation of the rift and spreading axis is controlled by the direction of external extension. This active–passive scenario corresponds to the *LIP-Producer* exemplified by the Deccan and Madagascar LIPs.

In addition, plumes can play a limited, yet important and sometimes even definitive role in the dynamics of plate rupture. These include (1) initiating break-up when rifting is already underway, thereby determining the timing of lithospheric rupture (*LIP-Trigger*, e.g., the CAMP and the Karoo LIP), and (2) creating mechanically soft zones in the lithosphere that spatially control the direction of propagation of oceanic spreading (*LIP-Attractor*, e.g., the Afar and Paraná–Etgedeka LIPs).

Two remaining types of LIPs are *LIP-Dornröschen* (Iceland plume) and *LIP-Sleeper* (Manus basin). This implies that interpretation of the timing of LIP emplacement made from a mantle dynamics perspective<sup>27</sup> should be handled with caution because of possible delays between the timing of upwelling in the mantle and its detectable magmatic manifestation at or near the Earth’s surface.

Although our classification is currently based on the best-known examples of continental Phanerozoic LIPs (Table 1), it should also be relevant to the future study of other LIPs (including Precambrian and oceanic), providing a generic guide for further studies of intraplate magmatism in terms of its relationship to plate rupture.

Received: 17 June 2023; Accepted: 20 December 2023;

Published online: 09 January 2024

## References

- Bryan, S. E. & Ernst, R. E. Revised definition of large igneous provinces (LIPs). *Earth-Sci. Rev.* **86**, 175–202 (2008).
- Bryan, S. E. & Ferrari, L. Large igneous provinces and silicic large igneous provinces: progress in our understanding over the last 25 years. *GSA Bull.* **125**, 1053–1078 (2013).
- Ernst, R. E. *Large Igneous Provinces* 666 (Cambridge University Press, 2014).
- Farnetani, C. G. & Richards, M. A. Numerical investigations of the mantle plume initiation model for flood basalt events. *J. Geophys. Res.: Solid Earth* **99**, 13813–13833 (1994).

5. Şengör, A. C., Ernst, R. E. & Buchan, K. L. Elevation as indicator of mantle-plume activity. Mantle plumes: their identification through time. *Geol. Soc. Am. Spec. Paper* **352**, 183–225 (2001).
6. Göğüş, O. H. Geodynamic experiments suggest that mantle plume caused Late Permian Emeishan Large Igneous Province in Southern China. *Int. Geol. Rev.* **64**, 375–389 (2022).
7. Campbell, I. H. & Griffiths, R. W. Implications of mantle plume structure for the evolution of flood basalts. *Earth Planet. Sci. Lett.* **99**, 79–93 (1990).
8. Campbell, I. H. Large igneous provinces and the mantle plume hypothesis. *Elements* **1**, 265–269 (2005).
9. Schubert, B. S., Bunge, H. P. & Ritsema, J. Tomographic filtering of high-resolution mantle circulation models: can seismic heterogeneity be explained by temperature alone? *Geochem. Geophys. Geosyst.* **10**, Q05W03 (2009).
10. Maguire, R., Ritsema, J., van Keken, P. E., Fichtner, A. & Goes, S. P- and S-wave delays caused by thermal plumes. *Geophys. J. Int.* **206**, 1169–1178 (2016).
11. Sobolev, S. V. et al. Linking mantle plumes, large igneous provinces and environmental catastrophes. *Nature* **477**, 312–316 (2011).
12. Dannberg, J. & Sobolev, S. V. Low-buoyancy thermochemical plumes resolve controversy of classical mantle plume concept. *Nat. Commun.* **6**, 6960 (2015).
13. Ritsema, J., Heijst, H. J. V. & Woodhouse, J. H. Complex shear wave velocity structure imaged beneath Africa and Iceland. *Science* **286**, 1925–1928 (1999).
14. Montelli, R., Nolet, G., Dahlen, F. A. & Masters, G. A catalogue of deep mantle plumes: new results from finite-frequency tomography. *Geochem. Geophys. Geosyst.* **7**, Q11007 (2006).
15. Morgan, W. J. Convection plumes in the lower mantle. *Nature* **230**, 42–43 (1971).
16. Cloetingh, S., Koptev, A., Lavecchia, A., Kovács, I. J. & Beekman, F. Fingerprinting secondary mantle plumes. *Earth Planet. Sci. Lett.* **597**, 117819 (2022).
17. Helffrich, G. R. & Wood, B. J. The Earth's mantle. *Nature* **412**, 501–507 (2001).
18. Koptev, A., Cloetingh, S. & Ehlers, T. A. Longevity of small-scale ('baby') plumes and their role in lithospheric break-up. *Geophys. J. Int.* **227**, 439–471 (2021).
19. Courtillot, V., Davaille, A., Besse, J. & Stock, J. Three distinct types of hotspots in the Earth's mantle. *Earth Planet. Sci. Lett.* **205**, 295–308 (2003).
20. Zhao, D., Yu, S. & Ohtani, E. East Asia: seismotectonics, magmatism and mantle dynamics. *J. Asian Earth Sci.* **40**, 689–709 (2011).
21. Kuritani, T., Ohtani, E. & Kimura, J. I. Intensive hydration of the mantle transition zone beneath China caused by ancient slab stagnation. *Nat. Geosci.* **4**, 713–716 (2011).
22. Kuritani, T. et al. Buoyant hydrous mantle plume from the mantle transition zone. *Sci. Rep.* **9**, 6549 (2019).
23. Klausen, M. B. Conditioned duality between supercontinental 'assembly' and 'breakup' LIPs. *Geosci. Front.* **11**, 1635–1649 (2020).
24. Heron, P. J. & Lowman, J. P. The effects of supercontinent size and thermal insulation on the formation of mantle plumes. *Tectonophysics* **510**, 28–38 (2011).
25. Coltice, N. et al. Global warming of the mantle beneath continents back to the Archaean. *Gondwana Res.* **15**, 254–266 (2009).
26. Courtillot, V., Jaupart, C., Manighetti, I., Tapponnier, P. & Besse, J. On causal links between flood basalts and continental breakup. *Earth Planet. Sci. Lett.* **166**, 177–195 (1999).
27. Doucet, L. S. et al. Coupled supercontinent–mantle plume events evidenced by oceanic plume record. *Geology* **48**, 159–163 (2020).
28. Ziegler, P. A. & Cloetingh, S. Dynamic processes controlling evolution of rifted basins. *Earth-Sci. Rev.* **64**, 1–50 (2004).
29. Buitter, S. J. & Torsvik, T. H. A review of Wilson Cycle plate margins: a role for mantle plumes in continental break-up along sutures? *Gondwana Res.* **26**, 627–653 (2014).
30. Foulger, G. R. & Anderson, D. L. A cool model for the Iceland hotspot. *J. Volcanol. Geotherm. Res.* **141**, 1–22 (2005).
31. Peace, A. L. et al. A review of Pangaea dispersal and Large Igneous Provinces—in search of a causative mechanism. *Earth-Sci. Rev.* **206**, 102902 (2020).
32. Foulger, G. R. & Hamilton, W. B. Plume hypothesis challenged. *Nature* **505**, 618–618 (2014).
33. Foulger, G. R. The plate theory for volcanism. In *Encyclopedia of Geology* Vol. 3 (eds Elias, S. & Alderton, D.) 879–890 (Academic Press, United Kingdom, 2021).
34. Coffin, M. F. & Eldholm, O. Large igneous provinces: crustal structure, dimensions, and external consequences. *Rev. Geophys.* **32**, 1–36 (1994).
35. Jackson, M. G., Konter, J. G. & Becker, T. W. Primordial helium entrained by the hottest mantle plumes. *Nature* **542**, 340–343 (2017).
36. Huismans, R. S., Podladchikov, Y. Y. & Cloetingh, S. Transition from passive to active rifting: relative importance of asthenospheric doming and passive extension of the lithosphere. *J. Geophys. Res.: Solid Earth* **106**, 11271–11291 (2001).
37. Burov, E. & Gerya, T. Asymmetric three-dimensional topography over mantle plumes. *Nature* **513**, 85–89 (2014).
38. Koptev, A., Calais, E., Burov, E., Leroy, S. & Gerya, T. Dual continental rift systems generated by plume–lithosphere interaction. *Nat. Geosci.* **8**, 388–392 (2015).
39. Koptev, A., Cloetingh, S., Gerya, T., Calais, E. & Leroy, S. Non-uniform splitting of a single mantle plume by double cratonic roots: insight into the origin of the central and southern East African Rift System. *Terra Nova* **30**, 125–134 (2018).
40. Reichow, M. K. et al. The timing and extent of the eruption of the Siberian Traps large igneous province: implications for the end-Permian environmental crisis. *Earth Planet. Sci. Lett.* **277**, 9–20 (2009).
41. Saunders, A. & Reichow, M. The Siberian Traps and the End-Permian mass extinction: a critical review. *Chin. Sci. Bull.* **54**, 20–37 (2009).
42. Nikishin, A. M., Ziegler, P. A., Abbott, D., Brunet, M. F. & Cloetingh, S. A. P. L. Permo-Triassic intraplate magmatism and rifting in Eurasia: implications for mantle plumes and mantle dynamics. *Tectonophysics* **351**, 3–39 (2002).
43. Saunders, A. D., England, R. W., Reichow, M. K. & White, R. V. A mantle plume origin for the Siberian traps: uplift and extension in the West Siberian Basin, Russia. *Lithos* **79**, 407–424 (2005).
44. Nemova, V. D. *Lithogenic Classification of Rocks and Technomorphism of the Deposits of the Bazhenov Formation of the West Siberian Petroleum Province*. Habilitation Thesis 342, Lomonosov Moscow State University (2021).
45. Nemova, V. *The Study of the Upper Jurassic Deposits of the West Siberian Basin is the Development of one Innovation*. A manual for those who want to work consciously and with the great pleasure. Monograph, 156 (MAKS Press, Moscow, 2023).
46. Chung, S. L. & Jahn, B. M. Plume-lithosphere interaction in generation of the Emeishan flood basalts at the Permian–Triassic boundary. *Geology* **23**, 889–892 (1995).
47. Shellnutt, J. G., Denyszyn, S. W. & Mundil, R. Precise age determination of mafic and felsic intrusive rocks from the Permian Emeishan large igneous province (SW China). *Gondwana Res.* **22**, 118–126 (2012).
48. Song, X. Y., Zhou, M. F., Cao, Z. M. & Robinson, P. T. Late Permian rifting of the South China Craton caused by the Emeishan mantle plume? *J. Geol. Soc.* **161**, 773–781 (2004).
49. Munteanu, M. et al. Panxi region (South-West China): tectonics, magmatism and metallogenesis. A review. *Tectonophysics* **608**, 51–71 (2013).
50. Wang, Y. et al. Rifting in SW China: structural and sedimentary investigation of the initial crustal response to emplacement of the Permian Emeishan LIP. *Geol. Mag.* **156**, 745–758 (2019).
51. Ziegler, P. A. & Dèzes, P. Evolution of the lithosphere in the area of the Rhine Rift System. *Int. J. Earth Sci.* **94**, 594–614 (2005).
52. Fekiacova, Z., Mertz, D. F. & Renne, P. R. Geodynamic setting of the tertiary Hoheifel volcanism (Germany), Part I: 40 Ar/39 Ar geochronology. In *Mantle Plumes: A Multidisciplinary Approach* (eds Ritter, J. R. & Christensen, U. R.) 185–206 (Springer, 2007).
53. Sobolev, S. V. et al. Upper mantle temperatures and lithosphere–asthenosphere system beneath the French Massif Central constrained by seismic, gravity, petrologic and thermal observations. *Tectonophysics* **275**, 143–164 (1997).
54. Ritter, J. R. The seismic signature of the Eifel plume. In *Mantle Plumes: A Multidisciplinary Approach* (eds Ritter, J. R. & Christensen, U. R.) 379–404 (Springer, 2007).
55. Séranne, M., Couëffé, R., Husson, E., Baral, C. & Villard, J. The transition from Pyrenean shortening to Gulf of Lion rifting in Languedoc (South France)—a tectonic-sedimentation analysis. *BSGF-Earth Sci. Bull.* **192**, 27 (2021).
56. Cucciniello, C., Morra, V., Melluso, L. & Jourdan, F. Constraints on duration, age and migration of the feeder systems of the Madagascan flood basalt province from high-precision 40Ar/39Ar chronology. *Geol. Soc. Lond. Special Publ.* **518**, 325–340 (2022).
57. Collier, J. S. et al. Age of Seychelles–India break-up. *Earth Planet. Sci. Lett.* **272**, 264–277 (2008).
58. Davies, G. F. Thermomechanical erosion of the lithosphere by mantle plumes. *J. Geophys. Res.: Solid Earth* **99**, 15709–15722 (1994).
59. Garcia-Castellanos, D., Cloetingh, S. & Van Balen, R. Modelling the Middle Pleistocene uplift in the Ardennes–Rhenish Massif: thermo-mechanical weakening under the Eifel? *Global Planet. Change* **27**, 39–52 (2000).
60. Heyn, B. H. & Conrad, C. P. On the relation between basal erosion of the lithosphere and surface heat flux for continental plume tracks. *Geophys. Res. Lett.* **49**, e2022GL098003 (2022).
61. Gerya, T. V., Stern, R. J., Baes, M., Sobolev, S. V. & Whattam, S. A. Plate tectonics on the Earth triggered by plume-induced subduction initiation. *Nature* **527**, 221–225 (2015).
62. Bahadori, A. & Holt, W. E. Geodynamic evolution of southwestern North America since the Late Eocene. *Nat. Commun.* **10**, 5213 (2019).
63. Koptev, A., Cloetingh, S., Kovács, I. J., Gerya, T. & Ehlers, T. A. Controls by rheological structure of the lithosphere on the temporal evolution of continental magmatism: inferences from the Pannonian Basin system. *Earth Planet. Sci. Lett.* **565**, 116925 (2021).

64. Zhu, R., Zhao, P. & Zhao, L. Tectonic evolution and geodynamics of the Neo-Tethys Ocean. *Sci. China Earth Sci.* **65**, 1–24 (2022).
65. Jagoutz, O., Royden, L., Holt, A. F. & Becker, T. W. Anomalous fast convergence of India and Eurasia caused by double subduction. *Nat. Geosci.* **8**, 475–478 (2015).
66. Coffin, M. F. & Rabinowitz, P. D. Evolution of the conjugate East African–Madagascar margins and western Somali Basin. *Geol. Soc. Am. Special Pap.* **226**, 77 (1988).
67. Ganerød, M. et al. Palaeoposition of the Seychelles microcontinent in relation to the Deccan Traps and the Plume Generation Zone in Late Cretaceous–Early Palaeogene time. *Geol. Soc. Lond. Special Publ.* **357**, 229–252 (2011).
68. Richards, M. A., Duncan, R. A. & Courtillot, V. E. Flood basalts and hot-spot tracks: plume heads and tails. *Science* **246**, 103–107 (1989).
69. Geogren, J. E., Lin, J. & Dick, H. J. Evidence from gravity anomalies for interactions of the Marion and Bouvet hotspots with the Southwest Indian Ridge: effects of transform offsets. *Earth Planet. Sci. Lett.* **187**, 283–300 (2001).
70. Longpré, M. A., Staudacher, T. & Stix, J. The November 2002 eruption at Piton de la Fournaise volcano, La Réunion Island: ground deformation, seismicity, and pit crater collapse. *Bull. Volcanol.* **69**, 511–525 (2007).
71. Fontaine, F. R. et al. Crustal and uppermost mantle structure variation beneath La Réunion hotspot track. *Geophys. J. Int.* **203**, 107–126 (2015).
72. Bredow, E., Steinberger, B., Gassmöller, R. & Dannberg, J. How plume–ridge interaction shapes the crustal thickness pattern of the Réunion hotspot track. *Geochem. Geophys. Geosyst.* **18**, 2930–2948 (2017).
73. Plummer, P. S. & Belle, E. R. Mesozoic tectono-stratigraphic evolution of the Seychelles microcontinent. *Sediment. Geol.* **96**, 73–91 (1995).
74. Plummer, P. S. The Amirante ridge/trough complex: response to rotational transform rift/drift between Seychelles and Madagascar. *Terra Nova* **8**, 34–47 (1996).
75. Biswas, S. K. Rift basins in western margin of India and their hydrocarbon prospects with special reference to Kutch basin. *AAPG Bull.* **66**, 1497–1513 (1982).
76. Biswas, S. K. Regional tectonic framework, structure and evolution of the western marginal basins of India. *Tectonophysics* **135**, 307–327 (1987).
77. Sheth, H. C. A historical approach to continental flood basalt volcanism: insights into pre-volcanic rifting, sedimentation, and early alkaline magmatism. *Earth Planet. Sci. Lett.* **168**, 19–26 (1999).
78. Guan, H., Geoffroy, L. & Xu, M. Magma-assisted fragmentation of Pangea: continental breakup initiation and propagation. *Gondwana Res.* **96**, 56–75 (2021).
79. Koptev, A. et al. Plume-induced continental rifting and break-up in ultra-slow extension context: insights from 3D numerical modeling. *Tectonophysics* **746**, 121–137 (2018).
80. Koptev, A., Calais, E., Burov, E., Leroy, S. & Gerya, T. Along-axis variations of rift width in a coupled lithosphere–mantle system, application to East Africa. *Geophys. Res. Lett.* **45**, 5362–5370 (2018).
81. Macgregor, D. History of the development of the East African Rift System: a series of interpreted maps through time. *J. Afr. Earth Sci.* **101**, 232–252 (2015).
82. Rogers, N. et al. Two mantle plumes beneath the East African rift system: Sr, Nd and Pb isotope evidence from Kenya Rift basalts. *Earth Planet. Sci. Lett.* **176**, 387–400 (2000).
83. Chang, S. J. & Van der Lee, S. Mantle plumes and associated flow beneath Arabia and East Africa. *Earth Planet. Sci. Lett.* **302**, 448–454 (2011).
84. Nelson, W. R., Furman, T., van Keken, P. E., Shirey, S. B. & Hanan, B. B. Os–Hf isotopic insight into mantle plume dynamics beneath the East African Rift System. *Chem. Geol.* **320**, 66–79 (2012).
85. Civiero, C., Lebedev, S. & Celli, N. L. A complex mantle plume head below East Africa–Arabia shaped by the lithosphere–asthenosphere boundary topography. *Geochem. Geophys. Geosyst.* **23**, e2022GC010610 (2022).
86. George, R., Rogers, N. & Kelley, S. Earliest magmatism in Ethiopia: evidence for two mantle plumes in one flood basalt province. *Geology* **26**, 923–926 (1998).
87. Coblenz, D. D. & Sandiford, M. Tectonic stresses in the African plate: constraints on the ambient lithospheric stress state. *Geology* **22**, 831–834 (1994).
88. Koptev, A. I. & Ershov, A. V. The role of the gravitational potential of the lithosphere in the formation of a global stress field. *Izv. Phys. Solid Earth* **46**, 1080–1094 (2010).
89. Min, G. & Hou, G. Geodynamics of the East African Rift System ~30 Ma ago: a stress field model. *J. Geodyn.* **117**, 1–11 (2018).
90. Müller, R. D., Gaina, C., Roest, W. R. & Hansen, D. L. A recipe for microcontinent formation. *Geology* **29**, 203–206 (2001).
91. Koptev, A. et al. Plume-induced breakup of a subducting plate: microcontinent formation without cessation of the subduction process. *Geophys. Res. Lett.* **46**, 3663–3675 (2019).
92. Stampfli, G. M. & Borel, G. D. A plate tectonic model for the Paleozoic and Mesozoic constrained by dynamic plate boundaries and restored synthetic oceanic isochrons. *Earth Planet. Sci. Lett.* **196**, 17–33 (2002).
93. Jolivet, L. Tethys and Apulia (Adria), 100 years of reconstructions. *C.R. Géosci.* **355**, 1–20 (2023).
94. Yang, G. Subduction initiation triggered by collision: a review based on examples and models. *Earth-Sci. Rev.* **232**, 104129 (2022).
95. Torsvik, T. H. Earth history: a journey in time and space from base to top. *Tectonophysics* **760**, 297–313 (2019).
96. Jolivet, L. et al. Neo-Tethys geodynamics and mantle convection: from extension to compression in Africa and a conceptual model for obduction. *Can. J. Earth Sci.* **53**, 1190–1204 (2016).
97. Marzoli, A. et al. Extensive 200-million-year-old continental flood basalts of the Central Atlantic Magmatic Province. *Science* **284**, 616–618 (1999).
98. Davies, J. H. F. L. et al. End-Triassic mass extinction started by intrusive CAMP activity. *Nat. Commun.* **8**, 15596 (2017).
99. Duncan, R. A., Hooper, P. R., Rehacek, J., Marsh, J. & Duncan, A. R. The timing and duration of the Karoo igneous event, southern Gondwana. *J. Geophys. Res.: Solid Earth* **102**, 18127–18138 (1997).
100. Jourdan, F. et al. Major and trace element and Sr, Nd, Hf, and Pb isotope compositions of the Karoo large igneous province, Botswana–Zimbabwe: lithosphere vs mantle plume contribution. *J. Petrol.* **48**, 1043–1077 (2007).
101. Jourdan, F., Féraud, G., Bertrand, H., Watkeys, M. K. & Renne, A. P. The 40Ar/39Ar ages of the sill complex of the Karoo large igneous province: implications for the Pliensbachian–Toarcian climate change. *Geochem. Geophys. Geosyst.* **9**, Q06009 (2008).
102. Svensen, H., Corfu, F., Polteau, S., Hammer, Ø. & Planke, S. Rapid magma emplacement in the Karoo large igneous province. *Earth Planet. Sci. Lett.* **325**, 1–9 (2012).
103. Favre, P. & Stampfli, G. M. From rifting to passive margin: the examples of the Red Sea, Central Atlantic and Alpine Tethys. *Tectonophysics* **215**, 69–97 (1992).
104. Le Roy, P. & Piqué, A. Triassic–Liassic Western Moroccan synrift basins in relation to the Central Atlantic opening. *Mar. Geol.* **172**, 359–381 (2001).
105. Luttinen, A. V. et al. Depleted mantle-sourced CFB magmatism in the Jurassic Africa–Antarctica rift: petrology and 40Ar/39Ar and U/Pb chronology of the Vestfjella Dyke Swarm, Dronning Maud Land, Antarctica. *J. Petrol.* **56**, 919–952 (2015).
106. Luttinen, A., Kurhila, M., Puttonen, R., Whitehouse, M. & Andersen, T. Periodicity of Karoo rift zone magmatism inferred from zircon ages of silicic rocks: implications for the origin and environmental impact of the large igneous province. *Gondwana Res.* **107**, 107–122 (2022).
107. Sibuet, J. C., Rouzo, S. & Srivastava, S. Plate tectonic reconstructions and paleogeographic maps of the central and North Atlantic oceans. *Can. J. Earth Sci.* **49**, 1395–1415 (2012).
108. Mueller, C. O. & Jokat, W. Geophysical evidence for the crustal variation and distribution of magmatism along the central coast of Mozambique. *Tectonophysics* **712**, 684–703 (2017).
109. Saki, M., Thomas, C., Nippress, S. E. & Lessing, S. Topography of upper mantle seismic discontinuities beneath the North Atlantic: the Azores, Canary and Cape Verde plumes. *Earth Planet. Sci. Lett.* **409**, 193–202 (2015).
110. Geldmacher, J., Hoernle, K., Bogaard, P. V. D., Duggen, S. & Werner, R. New 40Ar/39Ar age and geochemical data from seamounts in the Canary and Madeira volcanic provinces: support for the mantle plume hypothesis. *Earth Planet. Sci. Lett.* **237**, 85–101 (2005).
111. Beier, C., Haase, K.M., & Abouchami, W. Geochemical and geochronological constraints on the evolution of the Azores Plateau. In *Geological Society of America Special Papers* (eds Neal, C.R., Sager, W.W., Sano, T., & Erba, E.) 27–88 (The Geological Society of America, 2015).
112. Hastie, W. W., Watkeys, M. K. & Aubourg, C. Magma flow in dyke swarms of the Karoo LIP: implications for the mantle plume hypothesis. *Gondwana Res.* **25**, 736–755 (2014).
113. Bredow, E. & Steinberger, B. Variable melt production rate of the Kerguelen hotspot due to long-term plume–ridge interaction. *Geophys. Res. Lett.* **45**, 126–136 (2018).
114. Coffin, M. F. et al. Kerguelen hotspot magma output since 130 Ma. *J. Petrol.* **43**, 1121–1137 (2002).
115. Zhu, D. C. et al. The 132 Ma Comei–Bunbury large igneous province: remnants identified in present-day southeastern Tibet and southwestern Australia. *Geology* **37**, 583–586 (2009).
116. Gaina, C., Müller, R. D., Brown, B., Ishihara, T. & Ivanov, S. Breakup and early seafloor spreading between India and Antarctica. *Geophys. J. Int.* **170**, 151–169 (2007).
117. Williams, S. E., Whittaker, J. M., Granot, R. & Müller, D. R. Early India–Australia spreading history revealed by newly detected Mesozoic magnetic anomalies in the Perth Abyssal Plain. *J. Geophys. Res.: Solid Earth* **118**, 3275–3284 (2013).
118. Seton, M. et al. Global continental and ocean basin reconstructions since 200 Ma. *Earth-Sci. Rev.* **113**, 212–270 (2012).
119. Leroy, S. et al. From rifting to spreading in the eastern Gulf of Aden: a geophysical survey of a young oceanic basin from margin to margin. *Terra Nova* **16**, 185–192 (2004).

120. Ahmed, A. et al. Crustal structure of the rifted volcanic margins and uplifted plateau of Western Yemen from receiver function analysis. *Geophys. J. Int.* **193**, 1673–1690 (2013).
121. Hofmann, C. et al. Timing of the Ethiopian flood basalt event and implications for plume birth and global change. *Nature* **389**, 838–841 (1997).
122. Rooney, T. O. The Cenozoic magmatism of East-Africa: Part I—Flood basalts and pulsed magmatism. *Lithos* **286**, 264–301 (2017).
123. Gac, S. & Geoffroy, L. 3D Thermo-mechanical modelling of a stretched continental lithosphere containing localized low-viscosity anomalies (the soft-point theory of plate break-up). *Tectonophysics* **468**, 158–168 (2009).
124. Beniést, A., Koptev, A. & Burov, E. Numerical models for continental break-up: implications for the South Atlantic. *Earth Planet. Sci. Lett.* **461**, 176–189 (2017).
125. Moulin, M., Aslanian, D. & Unternehr, P. A new starting point for the South and Equatorial Atlantic Ocean. *Earth-Sci. Rev.* **98**, 1–37 (2010).
126. Stica, J. M., Zalán, P. V. & Ferrari, A. L. The evolution of rifting on the volcanic margin of the Pelotas Basin and the contextualization of the Paraná–Etendeka LIP in the separation of Gondwana in the South Atlantic. *Mar. Pet. Geol.* **50**, 1–21 (2014).
127. Franke, D. Rifting, lithosphere breakup and volcanism: comparison of magma-poor and volcanically rifted margins. *Mar. Pet. Geol.* **43**, 63–87 (2013).
128. Schettino, A., Macchiavelli, C., Pierantoni, P. P., Zaroni, D. & Rasul, N. Recent kinematics of the tectonic plates surrounding the Red Sea and Gulf of Aden. *Geophys. J. Int.* **207**, 457–480 (2016).
129. Darin, M. H. & Umhoefer, P. J. Diachronous initiation of Arabia–Eurasia collision from eastern Anatolia to the southeastern Zagros Mountains since middle Eocene time. *Int. Geol. Rev.* **64**, 2653–2681 (2022).
130. Abdelmalak, M. M. et al. Breakup volcanism and plate tectonics in the NW Atlantic. *Tectonophysics* **760**, 267–296 (2019).
131. Beniést, A., Koptev, A., Leroy, S., Sassi, V. & Guichet, X. Two-branch break-up systems by a single mantle plume: insights from numerical modeling. *Geophys. Res. Lett.* **44**, 9589–9597 (2017).
132. Steinberger, B., Bredow, E., Lebedev, S., Schaeffer, A. & Torsvik, T. H. Widespread volcanism in the Greenland–North Atlantic region explained by the Iceland plume. *Nat. Geosci.* **12**, 61–68 (2019).
133. Lundin, E. R. & Doré, A. G. NE Atlantic break-up: a re-examination of the Iceland mantle plume model and the Atlantic–Arctic linkage. *Geol. Soc. Lond. Pet. Geol. Conf. Ser.* **6**, 739–754 (2005).
134. Jakovlev, A. V., Bushenkova, N. A., Koulakov, I. Y. & Dobretsov, N. L. Structure of the upper mantle in the Circum-Arctic region from regional seismic tomography. *Russ. Geol. Geophys.* **53**, 963–971 (2012).
135. Lebedev, S., Schaeffer, A. J., Fullea, J. & Pease, V. Seismic tomography of the Arctic region: inferences for the thermal structure and evolution of the lithosphere. *Geol. Soc. Lond. Special Publ.* **460**, 419–440 (2018).
136. Celli, N. L., Lebedev, S., Schaeffer, A. J. & Gaina, C. The tilted Iceland Plume and its effect on the North Atlantic evolution and magmatism. *Earth Planet. Sci. Lett.* **569**, 117048 (2021).
137. Forsyth, D. A., Morel-AL’Huissier, P., Asudeh, I. & Green, A. G. Alpha Ridge and Iceland–products of the same plume? *J. Geodyn.* **6**, 197–214 (1986).
138. O’Neill, C., Müller, D. & Steinberger, B. On the uncertainties in hot spot reconstructions and the significance of moving hot spot reference frames. *Geochem. Geophys. Geosyst.* **6**, Q04003 (2005).
139. Doubrovine, P. V., Steinberger, B. & Torsvik, T. H. Absolute plate motions in a reference frame defined by moving hot spots in the Pacific, Atlantic, and Indian oceans. *J. Geophys. Res.: Solid Earth* **117**, B09101 (2012).
140. Saunders, A. D., Fitton, J. G., Kerr, A. C., Norry, M. J. & Kent, R. W. The North Atlantic Igneous Province. *AGU Geophys. Monogr.* **100**, 45–93 (1997).
141. Meyer, R., Van Wijk, J. & Gernigon, L. The North Atlantic Igneous Province: a review of models for its formation. *Geol. Soc. Am. Special Pap.* **430**, 525–552 (2007).
142. Storey, M., Duncan, R. A. & Tegner, C. Timing and duration of volcanism in the North Atlantic Igneous Province: implications for geodynamics and links to the Iceland hotspot. *Chem. Geol.* **241**, 264–281 (2007).
143. Chalmers, J. A., Larsen, L. M. & Pedersen, A. K. Widespread Palaeocene volcanism around the northern North Atlantic and Labrador Sea: evidence for a large, hot, early plume head. *J. Geol. Soc.* **152**, 965–969 (1995).
144. Chauvet, F. et al. Eocene continental breakup in Baffin Bay. *Tectonophysics* **757**, 170–186 (2019).
145. Lundin, E. & Doré, A. G. Mid-Cenozoic post-breakup deformation in the ‘passive’ margins bordering the Norwegian–Greenland Sea. *Mar. Pet. Geol.* **19**, 79–93 (2002).
146. Gernigon, L., Blischke, A., Nasuti, A. & Sand, M. Conjugate volcanic rifted margins, seafloor spreading, and microcontinent: insights from new high-resolution aeromagnetic surveys in the Norway Basin. *Tectonics* **34**, 907–933 (2015).
147. Rysgaard, S., Bendtsen, J., Mortensen, J. & Sej, M. K. High geothermal heat flux in close proximity to the Northeast Greenland Ice Stream. *Sci. Rep.* **8**, 1344 (2018).
148. Petrunin, A. G. et al. Heat flux variations beneath central Greenland’s ice due to anomalously thin lithosphere. *Nat. Geosci.* **6**, 746–750 (2013).
149. Rogozhina, I. et al. Melting at the base of the Greenland ice sheet explained by Iceland hotspot history. *Nat. Geosci.* **9**, 366–369 (2016).
150. Martos, Y. M. et al. Geothermal heat flux reveals the Iceland hotspot track underneath Greenland. *Geophys. Res. Lett.* **45**, 8214–8222 (2018).
151. Mordret, A. Uncovering the Iceland hot spot track beneath Greenland. *J. Geophys. Res.: Solid Earth* **123**, 4922–4941 (2018).
152. Buchan, K. L. & Ernst, R. E. Giant circumferential dyke swarms: catalogue and characteristics. In *Dyke Swarms of the World: A Modern Perspective* (eds Srivastava, R., Ernst, R. & Peng, P.) *Springer Geology* 1–44 (Springer, Singapore, 2019).
153. White, R. & McKenzie, D. Magmatism at rift zones: the generation of volcanic continental margins and flood basalts. *J. Geophys. Res.: Solid Earth* **94**, 7685–7729 (1989).
154. Maher, H. D. Jr Manifestations of the Cretaceous High Arctic large igneous province in Svalbard. *J. Geol.* **109**, 91–104 (2001).
155. Golonka, J. & Bocharova, N. Y. Hot spot activity and the break-up of Pangea. *Palaeogeogr. Palaeoclimatol. Palaeoecol.* **161**, 49–69 (2000).
156. Koptev, A., Cloetingh, S., Burov, E., François, T. & Gerya, T. Long-distance impact of Iceland plume on Norway’s rifted margin. *Sci. Rep.* **7**, 10408 (2017).
157. François, T., Koptev, A., Cloetingh, S., Burov, E. & Gerya, T. Plume–lithosphere interactions in rifted margin tectonic settings: inferences from thermo-mechanical modelling. *Tectonophysics* **746**, 138–154 (2018).
158. Sleep, N. H. Lithospheric thinning by midplate mantle plumes and the thermal history of hot plume material ponded at sublithospheric depths. *J. Geophys. Res.: Solid Earth* **99**, 9327–9343 (1994).
159. Sleep, N. H. Lateral flow of hot plume material ponded at sublithospheric depths. *J. Geophys. Res.: Solid Earth* **101**, 28065–28083 (1996).
160. Sleep, N. H. Lateral flow and ponding of starting plume material. *J. Geophys. Res.: Solid Earth* **102**, 10001–10012 (1997).
161. Bright, R. M., Amato, J. M., Denyszyn, S. W. & Ernst, R. E. U-Pb geochronology of 1.1 Ga diabase in the southwestern United States: testing models for the origin of a post-Grenville large igneous province. *Lithosphere* **6**, 135–156 (2014).
162. Ebinger, C. J. & Sleep, N. H. Cenozoic magmatism throughout east Africa resulting from impact of a single plume. *Nature* **395**, 788–791 (1998).
163. Ershov, A. V. & Nikishin, A. M. Recent geodynamics of the Caucasus–Arabia–east Africa region. *Geotectonics* **38**, 123–136 (2004).
164. Faccenna, C., Becker, T. W., Jolivet, L. & Keskin, M. Mantle convection in the Middle East: reconciling Afar upwelling, Arabia indentation and Aegean trench rollback. *Earth Planet. Sci. Lett.* **375**, 254–269 (2013).
165. Stuart, F. M., Ellam, R. M., Harrop, P. J., Fitton, J. G. & Bell, B. R. Constraints on mantle plumes from the helium isotopic composition of basalts from the British Tertiary Igneous Province. *Earth Planet. Sci. Lett.* **177**, 273–285 (2000).
166. Ziegler, P. A. *Evolution of the Arctic–North Atlantic and the Western Tethys*. (AAPG Memoir, United States, 1988).
167. Brekke, H., Sjulstad, H. L., Magnus, C. & Williams, R. W. Sedimentary environments offshore Norway—an overview. *Nor. Pet. Soc. Special Publ.* **10**, 7–37 (2001).
168. Peng, P. et al. Earth’s oldest hotspot track at ca. 1.8 Ga advected by a global subduction system. *Earth Planet. Sci. Lett.* **585**, 117530 (2022).
169. Camp, V. E., Pierce, K. L. & Morgan, L. A. Yellowstone plume trigger for Basin and Range extension, and coeval emplacement of the Nevada–Columbia Basin magmatic belt. *Geosphere* **11**, 203–225 (2015).
170. Hooper, P. R., Camp, V. E., Reidel, S. P. & Ross, M. E. The Columbia River Basalts and their relationship to the Yellowstone hotspot and Basin and Range extension. In *Plumes, Plates, and Planetary Processes: Geological Society of America Special Paper 430* (eds Foulger, G.R. & Jurdy, J.M.) 635–668 (Geological Society of America, 2007).
171. Camp, V. E. & Wells, R. E. The case for a long-lived and robust Yellowstone hotspot. *GSA Today* **31**, 4–10 (2021).
172. French, S. W. & Romanowicz, B. Broad plumes rooted at the base of the Earth’s mantle beneath major hotspots. *Nature* **525**, 95–99 (2015).
173. Chu, R., Leng, W., Helmberger, D. V. & Gurnis, M. Hidden hotspot track beneath the eastern United States. *Nat. Geosci.* **6**, 963–966 (2013).
174. Yang, T. & Leng, W. Dynamics of hidden hotspot tracks beneath the continental lithosphere. *Earth Planet. Sci. Lett.* **401**, 294–300 (2014).
175. Brune, S. et al. Geodynamics of continental rift initiation and evolution. *Nat. Rev. Earth Environ.* **4**, 235–253 (2023).
176. Brune, S., Corti, G. & Ranalli, G. Controls of inherited lithospheric heterogeneity on rift linkage: numerical and analog models of interaction between the Kenyan and Ethiopian rifts across the Turkana depression. *Tectonics* **36**, 1767–1786 (2017).
177. Corti, G. et al. Aborted propagation of the Ethiopian rift caused by linkage with the Kenyan rift. *Nat. Commun.* **10**, 1309 (2019).
178. Glerum, A., Brune, S., Stamps, D. S. & Strecker, M. R. Victoria continental microplate dynamics controlled by the lithospheric strength distribution of the East African Rift. *Nat. Commun.* **11**, 2881 (2020).

179. Muluneh, A. A. et al. Mechanism for deep crustal seismicity: insight from modeling of deformation processes at the Main Ethiopian Rift. *Geochem. Geophys. Geosyst.* **21**, e2020GC008935 (2020).
180. Mulibo, G. D. & Nyblade, A. A. Mantle transition zone thinning beneath eastern Africa: evidence for a whole-mantle superplume structure. *Geophys. Res. Lett.* **40**, 3562–3566 (2013).
181. Halldórsson, S. A., Hilton, D. R., Scarsi, P., Abebe, T. & Hopp, J. A common mantle plume source beneath the entire East African Rift System revealed by coupled helium–neon systematics. *Geophys. Res. Lett.* **41**, 2304–2311 (2014).
182. Fitton, J. G. Active versus passive continental rifting: evidence from the West African rift system. *Tectonophysics* **94**, 473–481 (1983).
183. Pearce, J. A., Ernst, R. E., Peate, D. W. & Rogers, C. LIP printing: use of immobile element proxies to characterize Large Igneous Provinces in the geologic record. *Lithos* **392**, 106068 (2021).
184. Koptev, A. et al. Contrasted continental rifting via plume–craton interaction: applications to Central East African Rift. *Geosci. Front.* **7**, 221–236 (2016).

### Acknowledgements

We gratefully acknowledge support from the Alexander von Humboldt Foundation and the International Lithosphere Program (ILP). We thank Richard Ernst and two anonymous reviewers for insightful reviews of our manuscript. We thank Bernhard Steinberger for providing the digital data used to visualize the lithospheric thickness and the reconstructed shoreline configuration in Fig. 3a.

### Author contributions

A.K. initiated the conceptual framework for this study, inspired by the geodynamic material collected by S.C. Both authors worked closely together at all stages of the development of the ideas presented and in writing the manuscript.

### Funding

Open Access funding enabled and organized by Projekt DEAL.

### Competing interests

The authors declare no competing interests.

### Additional information

**Supplementary information** The online version contains supplementary material available at <https://doi.org/10.1038/s43247-023-01191-9>.

**Correspondence** and requests for materials should be addressed to Alexander Koptev.

**Peer review information** *Communications Earth & Environment* thanks Richard Ernst, Leif Karlstrom, and Grace Shephard for their contribution to the peer review of this work. Primary Handling Editor: Joe Aslin. A peer review file is available.

**Reprints and permission information** is available at <http://www.nature.com/reprints>

**Publisher's note** Springer Nature remains neutral with regard to jurisdictional claims in published maps and institutional affiliations.



**Open Access** This article is licensed under a Creative Commons Attribution 4.0 International License, which permits use, sharing, adaptation, distribution and reproduction in any medium or format, as long as you give appropriate credit to the original author(s) and the source, provide a link to the Creative Commons license, and indicate if changes were made. The images or other third party material in this article are included in the article's Creative Commons license, unless indicated otherwise in a credit line to the material. If material is not included in the article's Creative Commons license and your intended use is not permitted by statutory regulation or exceeds the permitted use, you will need to obtain permission directly from the copyright holder. To view a copy of this license, visit <http://creativecommons.org/licenses/by/4.0/>.

© The Author(s) 2024